TEST ON A PRESSURE VESSEL WITH FLAWS OF DIFFERENT LENGTH AND COMPARISON OF THE RESULT OF SPECIMENS

D. Aurich, K. Wobst and H. Krafka*

Axial flaws of 100···453 mm length were cut in the high strength steel StE 460 as well as in the HAZ of a pressure vessel of 1500 mm diameter and a wall thickness of 40 mm with a jeweller saw. The vessel was pressurized up to a COD where a considerable stable crack growth could be supposed. Attaining the COD the pressure was dropped and a hollow auger specimen was taken including the crack tip in order to obtain the amount of crack growth. The results in terms of critical CTOD and $J_R(\Delta a)$ were compared with critical CTOD-values of 3-point bend specimens and wide-plate specimens as well as with J_R-curves of CT specimens with fatigue cracks as well as with saw cuts with and without side grooves.

INTRODUCTION

This work is part of a project entitled "Investigations on the assessment of safety against cleavage fracture of welded steel structures with the aid of the results on small specimens and wide plates". Results of small tensile specimens, wide plate specimens CCP as well as 3-point bend specimens SENB with various thicknesses, widths, notch angles and notch root radii were already published (1 - 6). Fig. 1 shows test parameters and results of the used specimens. The chemical composition and the mechanical properties of the test material StE 460 (German Standard) are plotted in Tab. 1. Furthermore two welded joints with heat inputs of 20 kJ/cm and 50 kJ/cm were tested (Table 2). Finally tests on pressure vessels had to be carried out in order to check the validity of a safety analysis based on elastic-plastic fracture mechanics using the test results of various specimens

* Federal Institute for Materials Testing (BAM)
D-1000 Berlin 45

TABLE 1 - Steel StE 460: Chemical composition (mass %) and mechanical properties at 20 °C

C	Si	Mn	P	S	Ni	V
0,17	0,28	1,52	0,009	0,009	0,62	0,18

Lower yield point R_{eL}	480	N/mm²
Ultimate tensile strength R_m	633	N/mm²
Elongation in % D A_5	23	%
Reduction of area Z	60	%
Charpy (upper shelf) energy A_v	135	J

TABLE 2 - Welded joints

Geometry	Double U 2/3 - 1/3
Welding process	Submerged arc
Wire	S_2Ni2,5(Ø 4 mm)
Flux	LW 330
Heat input	20 kJ/cm, 50 kJ/cm
Preheating temperature	175 °C ± 20 °C
Heat treatment	No
Retreatment	No straightening

The parameters of the pressure vessel tests were:

- type and size of flaws: through wall flaws or cracks respectively, semielliptical surface notches (cracks) of various dimensions,
- microstructure in the vicinity of the flawes: base metal and heat affected zone HAZ produced by 20 kJ/cm heat input,
- loading by internal pressure P : P until initiation or limited extension of a stable crack respectively.

PRESSURE VESSEL TESTS

The test temperature was 22 °C and the length ($2c_0$) of the through wall flaw varied from 100 mm to 453 mm, it was located in the base metal as well as in the HAZ 0,3 mm beside the fusion line of the 20 kJ/cm welded joint respectively. Criteria for crack initiation and limited stable crack growth were the crack tip opening displacement δ_t and the J-integral.

Fig. 2 shows the dimensions of the vessel. The flaws were located inside round I and II of 650 mm diameter, which were welded to the middle of the cylindrical part and alligned parallel to the vessel axis. At the end of a test procedure hollow auger specimens around the crack tip were taken for metallographic examination. Different flaw lengths were produced by extension of the slot by sawing after the tests. Fig. 3 demonstrates the dimensions and orientation of a flaw in the HAZ of the 20 kJ/cm welded joint. The significant parts of the flaw were the 0,2 mm wide slots on each side.

The following data were measured:
during the pressure test:
- internal pressure,
- notch opening displacement V in a distance of 3 mm from the notch tip,
- the strain distribution in front of the crack (notch) tip,
- test temperature

after the test:
- investigation of hollow auger specimens (diameter 10 mm) at the crack tip:
  - stable crack extension Δa as a function of the position in the vessel wall,
  - crack (notch) opening displacement and crack (notch) tip opening displacement as a function of the position in the vessel wall
  - notch position and crack extension in the HAZ-microstructure in the case of the welded joint.

RESULTS

Fig. 4 - 6 shows results obtained from hollow auger specimens. Flaw and crack contours were measured at least at 6 cross sections, which were prepared for metallographical examination. The crack (notch) opening displacement values were obtained at the notch tip as well as in a distance of 3 mm away from it.

Fig. 4 demonstrates stable crack extensions in the vessel wall in front of flaws of different length. It is remarkable, that for the same internal pressure crack growth on either side of the slot was different. Compare both curves for equal pressure 15,6 MPa and 18,6 MPa.

Fig. 5 shows the measuring procedure for the notch resp. crack tip displacement. For the determination of δ_t, the plastic and elastic parts of the notch (crack) tip displacements were added, whereby δ_e was obtained according to BS 5762 (7).

Fig. 6 demonstrates examples of the distributions of notch opening displacement V_o in the vessel wall. Again a different behavior at the two notch tips of a flaw is evident.

Fig. 7 and 8 compare the critical notch (crack) displacements at stable crack initiation obtained at T_i with SENB specimens (5), CCP specimens (6) and the pressure vessel. For SENB δ was determined in accordance to BS 5762 (7) and for CCP it was measured after the test.

Fig. 7a shows for SENB the interdependence of the critical notch (crack) tip opening displacement at T_i on the notch root radius. Obviously there is no influence of the notch position (T-L or T-S) on $(\delta_c)_{Ti}$. Fig. 7b compares the results of SENB, CCP and pressure vessel tests. There is a rather good agreement between the results of the vessel and SENB-tests whereas the results of the wide plate tests are different. The reason of the deviation is not quite clear. But it must be kept in mind, that for wide plates with an a/W-ratio of 0,08 the flaws were relatively small.

In Fig. 8 results obtained with welded joints notched in the HAZ 0,3 mm beside the fusion line are plotted. Compared to the base metal δ_c-values for stable crack initiation, the HAZ-values are smaller for the vessel as well as for the wide plate. Thus, the 20 kJ/cm welded joint seems to have somewhat lower δ_c-values than the base metal. Generally welded joint and base metal behave rather similar concerning initiation of stable cracks. The same statement is valid for the 50 kJ/cm welded joint with $(\delta_o)_{Ti}$-values only slightly above the base metal values (Fig. 8b).

In the following we compare results concerning J-integrals obtained with CT25-specimens, wide plates (6) as well as for the vessel.

Fig. 9 shows crack resistance plots which were determined with CT25-specimens of different dimensions according to ASTM E 813-81. Single specimen tests using a DC-potential method for crack extension measurement yielding comparable J_R-Δa-plots. The J_R-curves of specimens without side grooves were nearly identical, whereas side grooved specimens obviously had a different slope.

Fig. 10 again includes a comparison between CT25, wide plate and vessel tests concerning J_R- Δa-plots. Since the Δa-values of the vessel and wide plate tests are related exclusively to stable crack extension in the following diagramms, the J_R-curves of CT25-specimens were shifted 0,1 mm (width of the stretch zone) to the left.

$J_{applied}$ of the vessel was determined using the equation of Paris and Johnson (8) with β = 2:

$$J_I = \frac{R_{eL}^2}{E} \quad c \cdot \frac{\pi \, (P/P_k)^2}{1-1/\beta \, (P/P_k)^2} \qquad |1|$$

β = 2, plane stress condition
β = 6, plain strain condition

Fig. 10 shows that only one value of vessel tests 2 and 4 respectively deviates remarkable from J_R-curve of side grooved CT25-specimens. The J_R-Δa value of wide plates determined according to (9) yielded relatively large deviations in comparison to the other tests.

Fig. 11 shows the same functions as fig. 10 for a notch root position in the HAZ. Only the results of vessel tests 1 and 2 clearly lie below the reference curve of side grooved CT25-specimens. For these experiments the flaws were relatively short. Therefore it can be assumed, that residual stresses caused by shrinkage which had been produced during welding of the round were added to the circumferential stress produced by the internal pressure. It was estimated, that a tensile residual stress of 50 N/mm² would be sufficent to explain the observed deviations. Wether there are realy tensile residual stresses will be proofed by further tests. The J_R-Δa-value of the wide plate again is too high, but the deviation is smaller than for the notch position in the base metal (compare Fig. 10 and 11).

Fig. 12 gives a survey of J_R-values as a function of flaw length, determined by vessel tests with notch positions in the base metal and HAZ of the 20 kJ/cm welded joint. The hatched columns referred to J_R-values determined by the vessel tests with the aid of equation 1. The unhatched columns had been calculated by using the Δa-values of the vessel tests in connection with the J_R-curve of the side grooved base metal CT25-specimens. Assuming tensile residual stresses of 50 N/mm², the J_R-values would be increased as shown by arrows.

CONCLUSIONS

The results show, that values of initiation and extension of stable cracks determined with SENB-specimens and CT25-specimens can be transfered to vessel with through wall flaws. But with specimen values alone the assessment of the vessel behaviour is not very conservative.

In several cases wide plate tests (CCP) are not useful to simulate the behaviour of vessels with through wall flaws. The reason of this is not quite clear. Further experiments are necessary to find out wether increasing the a/W-ratio will improve the correspondence to the vessel tests. A further argument could be, that for wide plates crack initiation always occured after general yield, whereas for vessels initiation took place, below the limit load for plastic collapse.

ACKNOWLEDGEMENTS

This work is part of a project sponsered by the Deutsche Forschungsgemeinschaft DFG, ERP-Sondervermögen Berlin and the research foundation of the Verein Deutscher Eisenhüttenleute VDEh. Financial support is gratefully acknowleded. We also would like to thank the German steel plants for provision of the test material.

SYMBOLS USED

a, c	= notch length, crack length CCP, vessel: one-half the total length of notch resp. crack (mm)
Δa	= stable crack extension (mm)
A_v	= charpy energy (J)
B	= specimen thickness (mm)
BM	= base metal (StE 460)
CCP	= centre cracked tensile panel specimen
COD	= crack (notch) opening displacement (mm)
CTOD	= crack (notch) tip opening displacement (mm)
CT25	= compact specimen (ASTM E 813-81)
E	= Young's modulus (N/mm^2)
FL	= fusion line
HAZ	= heat affected zone of welded joint
J_I	= Rice's J-integral, modus I (N/mm)
J_R	= fracture resistance (N/mm)
P	= pressure (MPa)
Q	= heat input (kJ/cm)
R_{eL}	= lower yield point (N/mm^2)
s	= distance from external surface (mm)
SENB	= 3-point bend specimen with single edge notch
SG	= side grooves on CT-specimen (0,25B)
T	= temperature (°C)
T_i	= fibrous/cleavage transition temperature ($\Delta a \gtrless 0$ mm)
T-L, T-S	= crack (notch) plane orientation (ASTM E 399-81)
V	= crack (notch) opening displacement (mm)
W	= specimen width, CCP: one-half the total width (mm)
β	= numerical value
δ, δ_t	= crack tip opening displacement (mm)
ρ	= notch root radius (mm)

σ_E = tensile residual stress (N/mm^2)
2ω = notch angle (°)

Indices

c = critical value
e = elastic
i = at initiation of stable crack
k = at plastic collapse
p = plastic

REFERENCES

(1) Krafka, H., Wobst, K. and Ziebs, J., "Vorträge der 11. Sitzung des Arbeitskreises Bruchvorgänge", DVM Berlin, 1980, pp. 165 - 174

(2) Krafka, H., Wobst, K. and Aurich, D., "Vorträge der 12. Sitzung des Arbeitskreises Bruchvorgänge", DVM Berlin, 1981, pp. 373 - 381

(3) Krafka, H., Wobst, K., Ziebs, J. and Aurich, D., Preprints ICF5, Vol. 2, Pergamon Press Frankfurt, 1981, pp. 881 - 888

(4) Aurich, D., Arch. Eisenhüttenwesen, Vol. 53, No. 12, 1982, pp. 479 - 483

(5) Krafka, H., Wobst, K. and Aurich, D., Arch. Eisenhüttenwesen, Vol. 54, No. 6, 1983, pp. 245 - 252

(6) Aurich, D., Wobst, K. and Krafka, H., Stahl und Eisen, Vol. 104, No. 19, 1984, pp. 977 - 982

(7) British Standards BS 5762, 1972, "Methods for Crack Opening Displacement(COD)Testing"

(8) Paris, P.C. and Johnson, R.E., ASTM STP 803, Vol. 2, 1983, pp. 5 - 39

(9) Rice, J.R., Paris, P.C. and Merkle, J.G., ASTM STP 536, 1973, pp. 231 - 245

Specimen type	Test parameters					Results					
	B mm	W mm	a;c mm	ω °	ρ mm	T_i	δ_i	$\Delta a(T)$	J_i or J_{Ic}	$J_R(\Delta a)$	Rem
ISO-V	10	10	2	45	0,25	+		+	$J_{0,2}$	+	A_v, $A_{v\,inst}$
SENB	40	40	10	45	0,1-1,0	+	+	+			
		120	35	0	0;0,1	+	+	+			
		200	60	0	0;0,1	+	+	+			
CT	25	50	30	0	0;0,1				J_{Ic}	+	
CCP	40	185	15	0	0,1	+	+	+	* J_i		
Vessel	40		50-226	0	0,1		+		* J_i	+	

Figure 1 Investigated specimens and results

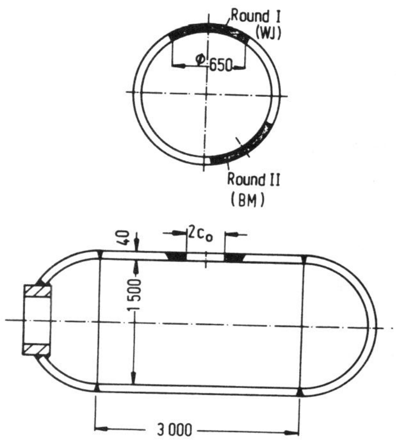

Figure 2 Test vessel

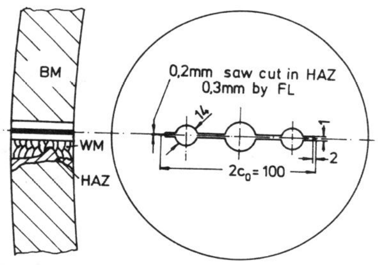

Figure 3 Round I, flaw in HAZ

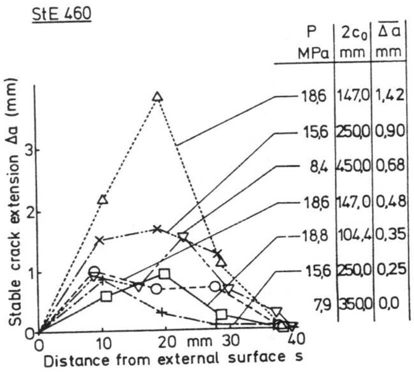

Figure 4 Stable crack extension in the vessel wall

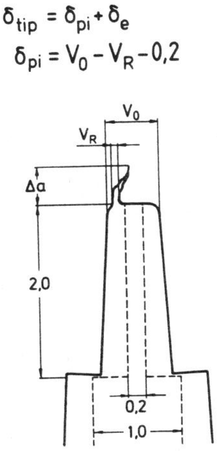

Figure 5 Determination of CTOD resp. δ_t

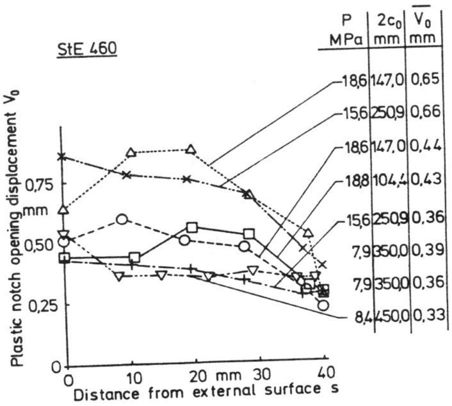

Figure 6 Notch root opening displacement in the vessel wall

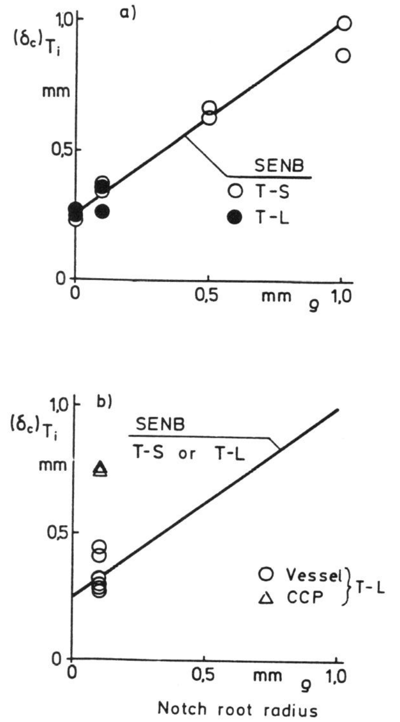

Figure 7 StE 460: Critical values of crack opening displacement vs. notch root radius

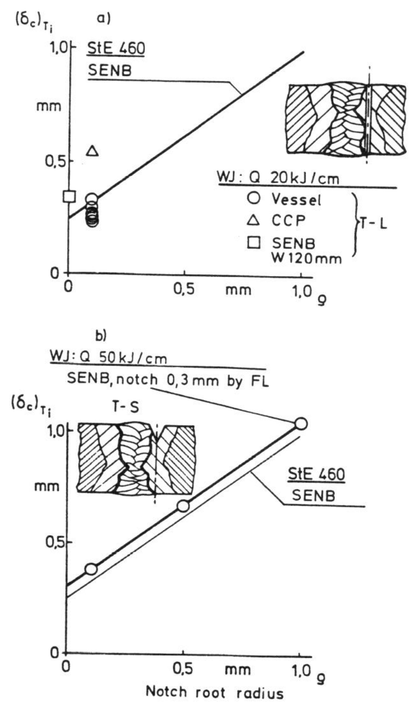

Figure 8 StE 460, notch root in HAZ 0,3 mm by FL: Critical values of crack opening displacement vs. notch root radius

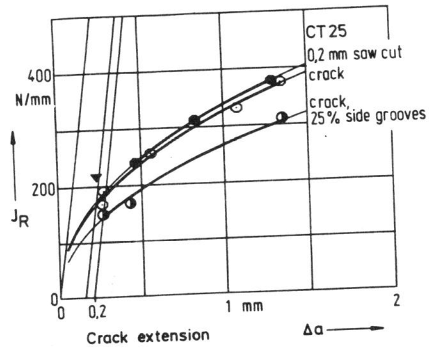

Figure 9 StE 460: $J_R(\Delta a)$-curves measured at 25 °C

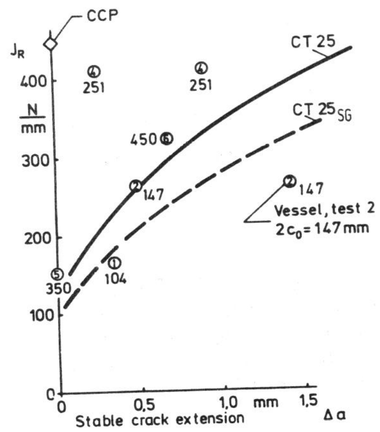

Figure 10 StE 460: $J_R(\Delta a)$-values of different specimens

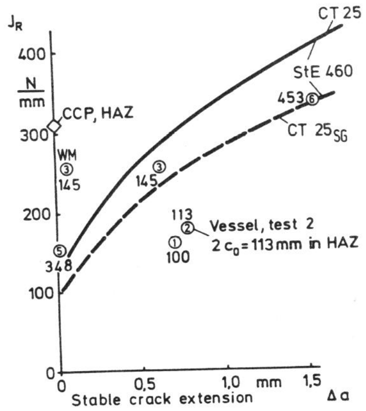

Figure 11 $J_R(\Delta a)$-values of different specimens

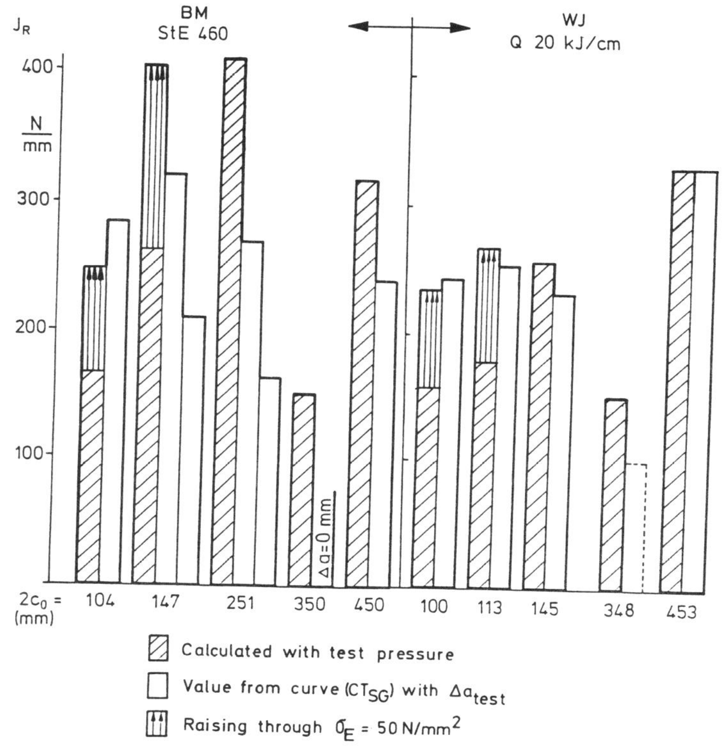

Figure 12 J_R-values of the vessel with flaw length $2c_o$